



## The evolving landscape and climate of western Flores: an environmental context for the archaeological site of Liang Bua

K.E. Westaway<sup>a,\*</sup>, R.G. Roberts<sup>a</sup>, T. Sutikna<sup>b</sup>, M.J. Morwood<sup>a,c</sup>, R. Drysdale<sup>d</sup>, J.-x. Zhao<sup>e</sup>, A.R. Chivas<sup>a</sup>

<sup>a</sup> GeoQuEST Research Centre, School of Earth and Environmental Sciences, University of Wollongong, Wollongong, NSW 2522, Australia

<sup>b</sup> Indonesian Centre for Archaeology, Jl. Raya Condet Pejaten No. 4, Jakarta 12001, Indonesia

<sup>c</sup> Archaeology and Palaeoanthropology, School of Human and Environmental Studies, University of New England, Armidale, New South Wales 2351, Australia

<sup>d</sup> School of Environmental and Life Sciences, Geology Building, University of Newcastle, Callaghan Campus, University Drive, Callaghan, NSW 2308, Australia

<sup>e</sup> Radiogenic Isotope Laboratory, Centre for Microscopy and Microanalysis, Department of Earth Sciences, University of Queensland, Brisbane, QLD 4072, Australia

### ARTICLE INFO

#### Article history:

Received 18 January 2008

Accepted 11 January 2009

#### Keywords:

Landscape evolution

Environmental context

Palaeoclimate changes

Geochronology

Geomorphological reconstruction

### ABSTRACT

The rapidly changing landscape of the eastern Indonesian archipelago has evolved at a pace dictated by its tropical climate and its geological and tectonic history. This has produced accelerated karstification, flights of alluvial terraces, and complex, multi-level cave systems. These cave systems sometimes contain a wealth of archaeological evidence, such as the almost complete skeleton of *Homo floresiensis* found at the site of Liang Bua in western Flores, but this information can only be understood in the context of the geomorphic history of the cave, and the more general geological, tectonic, and environmental histories of the river valley and region. Thus, a reconstruction of the landscape history of the Wae Racang valley using speleothems, geological structure, tectonic uplift, karst, cave, and terrace development, provides the necessary evidence to determine the formation, age, evolution, and influences on the site. This evidence suggests that Liang Bua was formed as two subterranean chambers ~600 ka, but could not be occupied until ~190 ka when the Wae Racang wandered to the southern side of the valley, exposing the chamber and depositing alluvial deposits containing artifacts. During the next ~190 k.yr., the chambers coalesced and evolved into a multi-level and interconnected cave that was subjected to channel erosion and pooling events by the development of sinkholes. The domed morphology of the front chamber accumulated deep sediments containing well stratified archaeological and faunal remains, but ponded water in the chamber further prevented hominin use of the cave until ~100 ka. These chambers were periodically influenced by river inundation and volcanic activity, whereas the area outside the cave was greatly influenced by glacial phases, which changed humid forest environments into grassland environments. This combined evidence has important implications for the archaeological interpretation of the site.

© 2009 Elsevier Ltd. All rights reserved.

### Introduction

The complex, dynamic, and often violent landscapes and environments that characterize the Indonesia region (Fig. 1a) have been formed by an amalgamation of interacting geological, tectonic, eustatic, and climatic processes (Audley-Charles, 1981; Simandjuntak and Barber, 1996; Hisheh et al., 1998; Kershaw et al., 2001). The movement of tectonic plates in this region created a converging plate margin, as the Indian Plate was subducted beneath the Eurasian Plate (Audley-Charles, 1981; Simandjuntak and Barber, 1996) (Fig. 2). This initiated submarine volcanism, causing the uplift and emergence of new crust (Hall, 1996, 2001), and is the driving

force behind the formation of the Banda Volcanic Arc, a string of volcanoes and volcanic islands that make up the Indonesian archipelago (Bellwood, 1997; Hall, 2002) (Fig. 1a).

The archipelago is located in a dynamic climatic zone, where the world's warmest sea water (the Indo Pacific warm pool or IPWP; Fig. 1) drives some of the globe's most significant atmospheric circulation systems, such as the Hadley and Walker circulation cells. The differential heating of the land and water causes the movement of the intertropical convergence zone (ITCZ) (Tapper, 2002), and drives the Asian monsoon system.

Deformation of the subducting plate also formed deep ocean trenches (Simandjuntak and Barber, 1996) (Fig. 2), which influenced the geodiversity and biodiversity of its many islands (Hall, 2002). For example, when emerging islands such as Flores (Fig. 1c) were surrounded by these trenches, they became permanently isolated from the mainland (continental landmasses of Asia – Sunda and

\* Corresponding author.

E-mail address: [kira@els.mq.edu.au](mailto:kira@els.mq.edu.au) (K.E. Westaway).

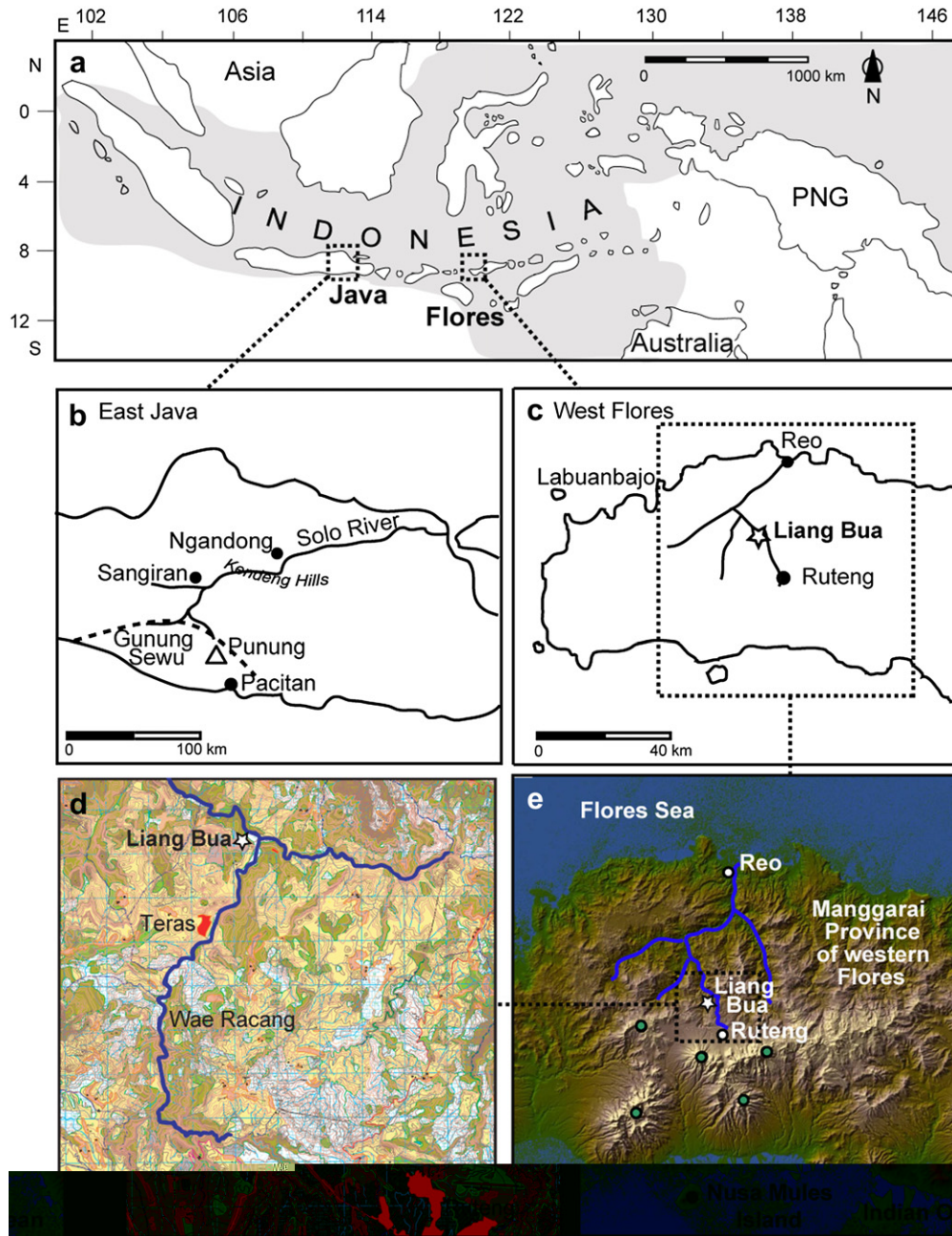


**Figure 1.** The Indonesian archipelago (a) showing the location of western Flores and eastern Java (dashed boxes). The dark shading represents the limits of the Indo Pacific warm pool. (b) Eastern Java showing the location of Punung (triangle) in the Gunung Sewu Southern Mountains (dashed line). (c) Western Flores showing the location of Ruteng and Liang Bua (white star). (d) A landsat image of western Flores and the study region, and (e) a topographic map of the same region from Ruteng to Liang Bua (white star). The main focus of this research is Liang Bua, but a sample for palaeoclimate analysis has been collected from a cave site near Punung in East Java.

Greater Australia – Sahul), even during periods of glacially lowered sea levels.

Flores is located in the middle of the Banda volcanic arc, at the heart of the Indonesian archipelago and IPWP (Fig. 1a). The initial volcanism that created the island was submarine (Burrett et al., 1991), which caused the rapid uplift of reefal limestone that surrounds the arc to form an active land surface. The rapidly evolving, tectonically active nature of Flores has resulted in unique landscapes of stepped alluvial terraces, multi-level cave systems, and well-developed surface karst features that are subjected to fluctuating climatic conditions (Fig. 3). The area around Liang Bua, near Ruteng in the mountainous Manggarai province, is a prime example of such a landscape.

Liang Bua is a large limestone chamber situated at the same elevation as the highest of three alluvial terraces (510 m a.m.s.l.), which were deposited by the Wae Racang river (Fig. 3g) in the wide Wae Racang valley composed of Miocene limestone (Fig. 3b–e). This site has accumulated a wealth of archaeological material during a ~100 k.yr. occupation period, including the almost complete skeleton of *Homo floresiensis* (Morwood et al., 2004, 2005). Despite the site's importance, essential Quaternary research in this region has been limited (Flenley, 1997; Dam et al., 2001) and little attention has been paid to the environmental factors that aided or impeded human dispersal in the region (Dennell, 2004). Consequently, a geological and environmental context for this site is lacking.

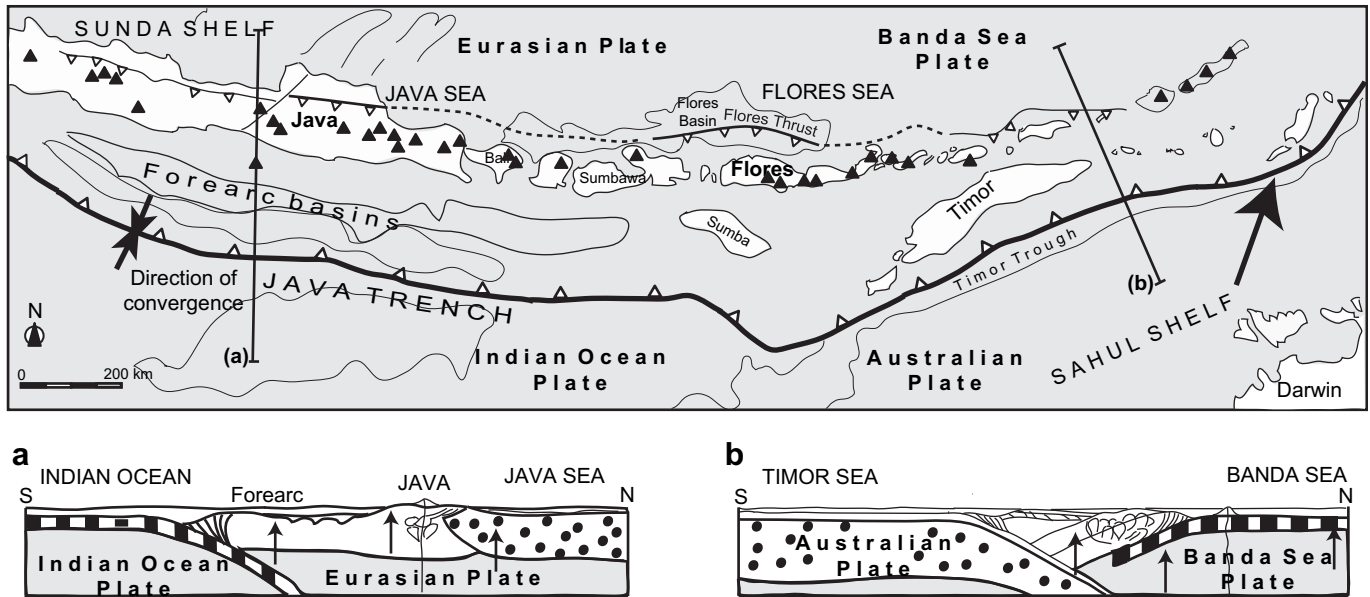


**Figure 2.** Subduction in the Indonesian archipelago: the collision zone between the Indian and Eurasian plates (left side) and southern Banda Arcs and Australia (right side). The subduction zone is represented by the deep Java Trench (open triangles) and the volcanic arc by the profusion of volcanoes (filled triangles). The transects relate to the subduction profiles (insets) for (a) Sunda shelf and (b) Banda Sea. The vertical arrows depict tectonic uplift. Redrawn from Hamilton (1979) and Simandjuntak and Barber (1996).

The aim of this paper is to reconstruct the geological, environmental, and landscape evolutionary history of the Wae Racang river valley. We will derive information from: speleothem records, the geological framework, tectonic uplift, and the evolution of the landscape using karst, cave, and terrace development, and will synthesize all the available evidence, including published and new data. This information will have implications for the interpretation of the site and its associated archaeological material by determining: 1) the formation of the site, 2) the age of the site, pre- and post-exposure, 3) the evolution of the site, and 4) the influences on the site (e.g., geomorphological, volcanic, and palaeo-environmental).

Therefore, this paper has been divided into four corresponding sections with results, discussion, and assessment of archaeological implications. The methods appropriate to each technique and a basic explanation of the interpretations can be found in the [supplementary online material \(SOM\)](#). In addition, the final summary combines the reconstructions and establishes the overall implications for the interpretation of the site, artifacts, and hominin remains.

### The formation of the site

Liang Bua was formed in a tectonically active karst region of western Flores. The key to understanding how the cave was formed lies in its weak geological structure, the dominance of tectonic uplift, rapid karstification, and the development of subterranean chambers in this region.

#### Weak geological structure

The volcanic spine of Flores was surrounded by large basins during the Middle Miocene, and sediments were sub-aqueously deposited to form sandstones and limestones, which were mixed with breccias and magmas from volcanic activity (van Bemmelen, 1949; Koesoemadinata et al., 1994; Monk et al., 1997). The limestone near Ruteng (Waihekeng Formation) is a tuff-bearing clastic limestone with a sandy composition, minimal compactness, and is of Pliocene-Miocene age (van Bemmelen, 1949). It is surrounded on all sides by a volcanic geology of tuffs and older volcanics (Fig. 3a). It

has a bedding thickness of  $\sim 700$  m and contains fragments of orange chert and fossils, which confirm that deposition occurred in a deep-sea environment (Koesoemadinata et al., 1994). Despite its bedding thickness, this limestone is minimally compact, weak, and porous (Fig. 4), which makes it particularly susceptible to rapid karstification, such as solution and the formation of subterranean chambers.

#### The dominance and rate of tectonic uplift

The subduction of tectonic plates causes large regions of the continental crust to be uplifted (e.g., Simandjuntak and Barber, 1996; Kopp et al., 2006). Since the early Pleistocene, the Miocene limestone beds of western Flores have been periodically uplifting to form land and create its present relief (Koesoemadinata et al., 1994). Evidence of this uplift can be seen in the coral-reef exposures along the south coast, such as on Nusa Mules Island (Fig. 1c, e), in the raised coral-reef terraces along the north coast, and on the neighboring islands of Sumba, Timor, Atauro, and Alors. These coral terraces provide the most reliable proxy for estimating uplift rates, but as very little analysis has been conducted on the terraces of Flores, the rate of tectonic uplift has been derived from raised coral-reef terraces from Cape Laundi, Sumba, which are located 75 km from the terraces on the south coast of Flores, and only 95 km from Ruteng. Dated by U-series techniques, the terraces span the last 1 Ma, providing an estimated uplift rate of between 0.2–0.5 mm/yr (Pirazzoli et al., 1991, 1993; Bard et al., 1996). This agrees with the estimation of 0.47 mm/yr for Atauro (Abbott and Chamalaun, 1981) and 0.03–0.5 mm/yr for Timor (Chappell and Veeh, 1978), which are also from the U-series dating of corals. Due to the proximity of these features to western Flores and the presence of similar coral reef terraces surrounding the island, it has been assumed that this rapid rate of uplift is also applicable to the study region and has resulted in rapid karstification.

#### Rapid karstification

When limestone is uplifted, its porous structure allows the creation of a series of cracks, which develop into passages and

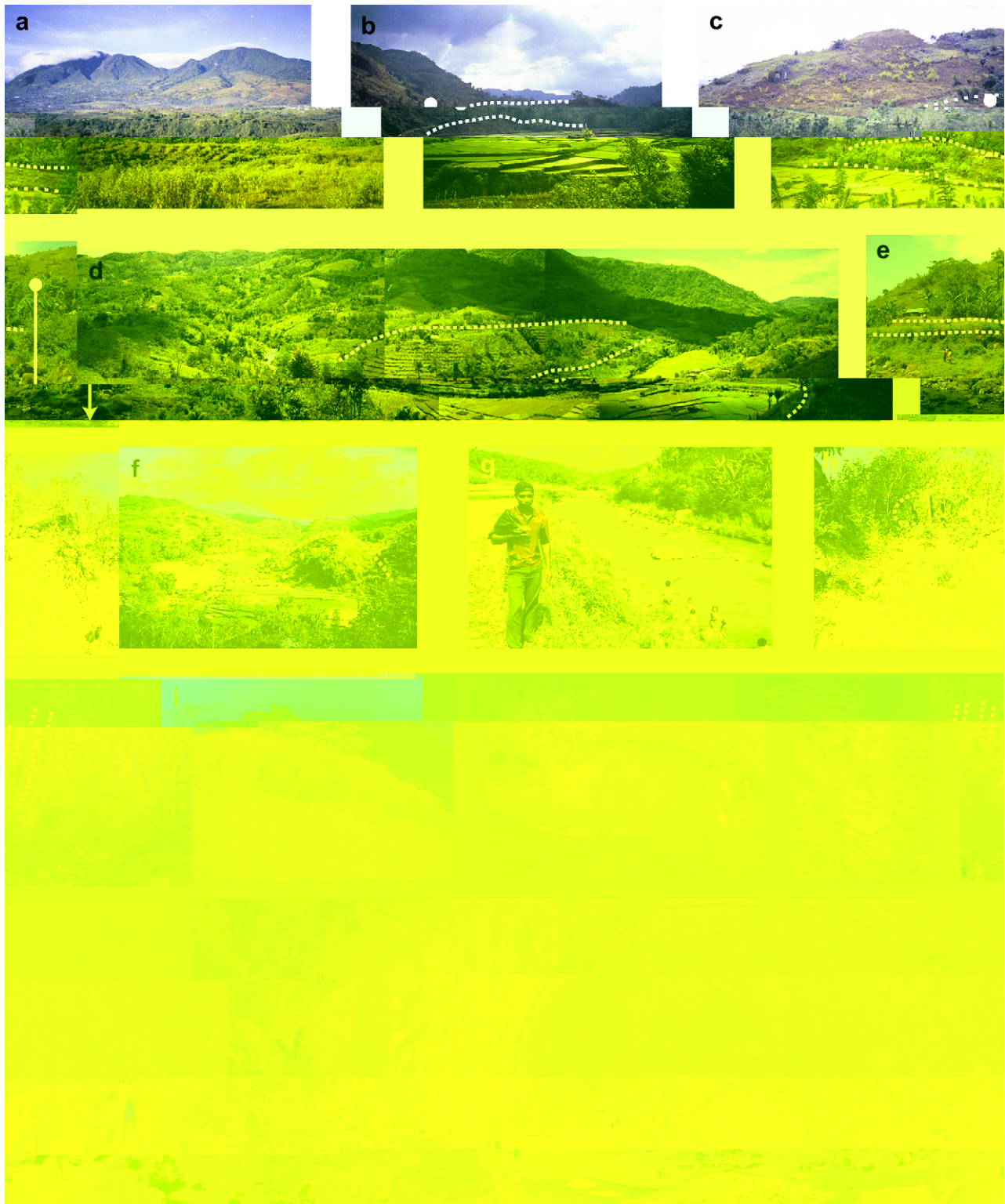


**Figure 3.** The environment within the vicinity of Liang Bua. (a) The volcanoes behind the town of Ruteng 14 km from Liang Bua. (b, c) Wae Racang valley (looking west and south, respectively) showing the location of the cave (white dot) and terraces (white dashed lines). (d) A panoramic view of Liang valley from above the cave (looking north-east) showing prominent terraces (white dashed lines) on the northern side of the valley. (e) The height of the cave (white dot) above the present river (white arrow) with the terraces (white dashed lines) in between. (f) External karst features, such as a karst cone (white dashed line) in Wae Racang valley. (g) The Wae Racang river close to the cave. (h) The composition of the third alluvial terrace (T1), which is capped by pyroclastic boulders (dashed white circles). (i) Liang Bua Outcrop I directly above the cave, and (j) the subterranean chamber directly below the cave. (k) Stalagmite SPJ3 from Java. (l) The pattern of stalagmite precipitation in Liang Bua, the stalagmites to the left (red dashed lines) have been affected by exposure while the stalagmites to the right (black dashed lines) have not. The conglomerate deposit has been marked with a white cross. (m) A panoramic view of Liang Bua (facing south) showing the shape of the domed front and elliptical rear chambers (dashed white lines) and the location of the conglomerate deposit (white cross).

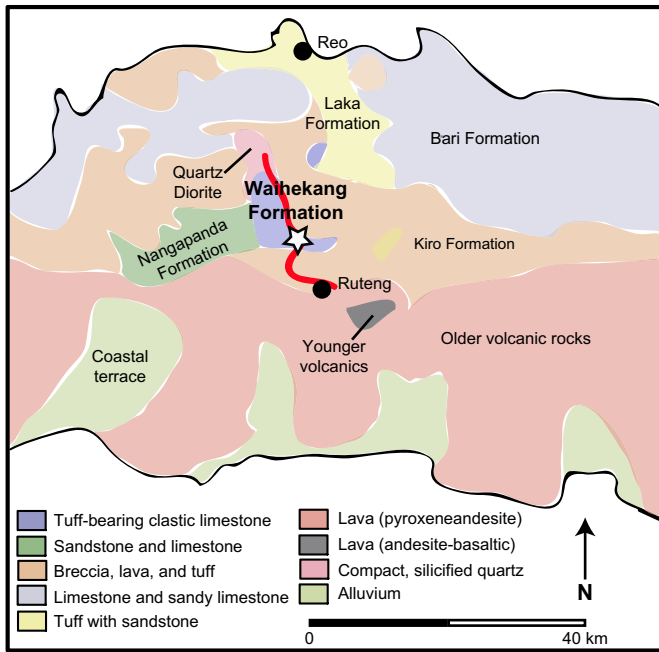


**Figure 4.** The geological framework for western Flores, showing the main lithology. The locations of Ruteng and Reo have been marked with a solid circle, and the path of the Wae Racang and location of Liang Bua have been marked with a red line and white star, respectively. Redrawn from Koesoemadinata et al. (1994).

chambers by the process of solution. A rapid rate of uplift will intensify the process of karstification by lowering the water table, which exposes more limestone to solution. In the Manggarai region, the extent of karstification mainly reflects lithological influences; soft, impure, tuff-bearing clastic limestones facilitate high densities of karst features, such as tall limestone cones, deep basins (dolines), and caves (Fig. 3f, j).

### The development of subterranean chambers

This area contains many dense cave systems, creating a honeycomb effect in the rounded limestone mountains. The Liang Bua cave system consists of two large dissolution chambers, Liang Bua and Liang Tanah; two remnant cave outcrops stacked above Liang Bua, Liang Bua Outcrop I and II (Fig. 3i); a large subterranean cave situated roughly 22 m below Liang Bua (Fig. 3j); and the Liang Jama collapsed cave system, found on the other side of the Liang Bua Mountain (Fig. 5). The caves below and above Liang Bua provide a context for its past and future development. The subterranean chamber is connected to Liang Bua by a series of sinkholes and still lies ~20 m below the land surface. In contrast, the outcrops above Liang Bua are situated 93 m and 75 m above the cave entrance, and presently comprise large blocks of weathered and dissolved limestone with evidence of remnant speleothems that have been dated to ~90 ka (sample SP1-TB [Fig. 5] and Roberts et al., 2009). This suggests that these features were operating as caves similar to Liang Bua ~90 ka, and have been successively elevated relative to the land surface by tectonic uplift.

The distribution of dolines and caves within this landscape and the structure of the Liang Bua cave system suggest that Liang Bua was formed as a subterranean chamber directly below a large doline by the process of solution. As such features represent the valleys in karst landscapes, this doline supplied the necessary slow-pewash water to enable solution to occur. It is possible that when Liang Bua formed, it developed as two subterranean chambers that later coalesced into one large cave, as suggested by the different forms of the rear (elliptical) and front (domed) chambers (Fig. 3m). As uplift continued, these subterranean chambers evolved into a multi-level and interconnected cave system that was progressively raised towards the land surface.

### Implications for the archaeology of Liang Bua

Subterranean chambers are seldom occupied due to the lack of access and the unwillingness of hominins to venture far into damp,

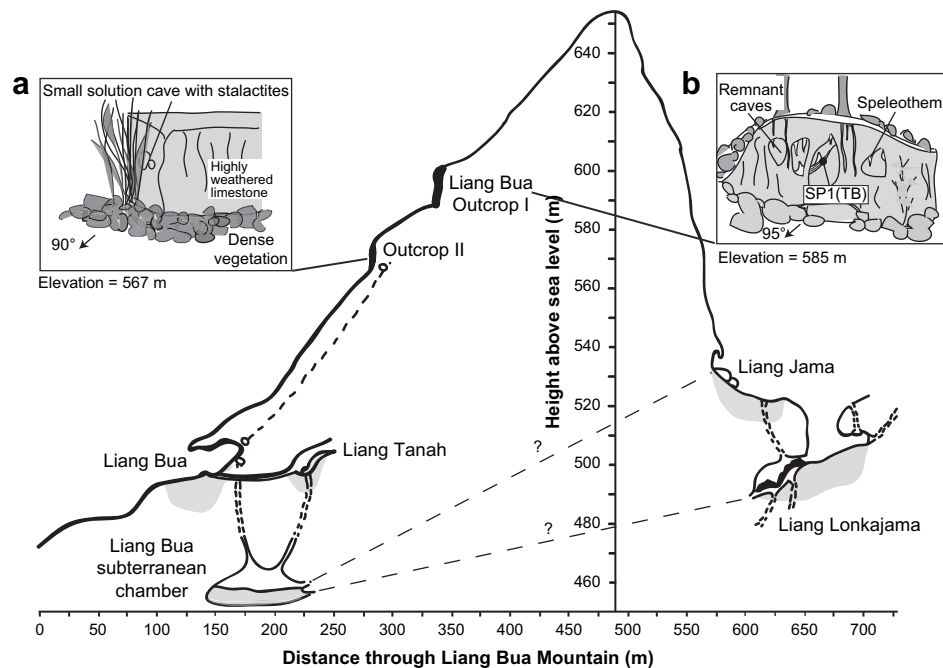


**Figure 5.** A profile through Liang Bua Mountain showing the multi-level and interconnected nature of the cave system. The inferred connections to the Liang Jama cave system have been marked with a dashed line, and the section drawings (insets a and b) describe the two outcrops above Liang Bua. Inset b also contains the location of flowstone sample SP1-TB (see text for details).

dark caves. Therefore, the formation of Liang Bua as a subterranean chamber represents a period of relative inactivity from an archaeological perspective. However, the details of its formation assist in determining the age of the site and the evolution of Liang Bua into its present form.

### **The age of the site**

As Liang Bua was formed as a subterranean chamber, the age of the site can be divided into two events, the formation age and the exposure age. The age of the former is of interest for understanding the geological and karstic evolution of the region, while the latter is of interest for the archaeological interpretation of the site as it provides a maximum age for occupation.

#### *Age of cave formation*

The age of a large flowstone block from Liang Bua (sample LB-17-A2) provides an indication of when the cave was formed. The flowstone, found in Sector III, yielded an age of  $374 \pm 30$  ka (Roberts et al., 2009), which suggests that the cave must have been in operation by at least  $\sim 400$  ka. Using this evidence, and a number of assumptions, we have estimated the age of cave formation. The assumptions are as follows: 1) the highest relief in this region is at  $\sim 820$  m (Golo Dukut); 2) the rate of uplift is 0.5 mm/yr (Pirazzoli et al., 1991, 1993; Bard et al., 1996); 3) the Miocene limestone originated at sea level and has been consistently uplifting; 4) karstification was initiated when uplift first occurred and the limestone was sub-aerially exposed; and 5) the falling water table kept pace with the rate of uplift. According to these assumptions, the uplift of this region occurred in the Early Pleistocene ( $\sim 1.5$  Ma) and the subterranean chamber of Liang Bua was formed by at least  $\sim 600$  ka. This estimate agrees with the age of the flowstone block, the rate of uplift, and the pace of karstification in this region.

#### *Age of cave exposure*

The sub-aerial exposure of Liang Bua created the first opportunity for human occupation. Evidence for when this event occurred can be gained from: 1) the age of the adjoining river terraces; 2) the pattern of cave collapse; and 3) the age of alluvial deposits found in the cave.

The age of the stepped river terraces The Wae Racang flows for  $\sim 25$  km from the slopes of Ruteng town north to the sea at Reo, and represents a smaller tributary of a much larger river system. Tectonic uplift in this region has triggered rapid river downcutting and the abandonment of the original floodplain, creating a series of at least three stepped alluvial terraces (Fig. 6 and Table 1). As Liang Bua is located on the first alluvial terrace, the formation and age of these geomorphic features provide evidence for the location of the river and the age of cave exposure.

The first alluvial terrace has been extensively eroded by river action in the vicinity of Liang Bua and has suffered limestone collapse, preserving only a remnant of its original extent. Its preservation is more extensive up valley, on the road to Teras, and down valley, past Liang Tanah (Fig. 6). On the northern side of the valley, the third terrace is extensive, with only a dry valley running westwards to interrupt its form. The second alluvial terrace is most apparent in front of Liang Bua, where it laterally extends for 62 m along the flanks of the river valley, and can be traced both up the river, towards the Wae Mulu and the limestone gorge, and down river, to a watering hole. This highly weathered terrace deposit is

**Table 1**  
The three alluvial terraces of the Wae Racang valley within the vicinity of Liang Bua.

Terrace	Elevation (m)	Form	Sedimentology	Color	Clasts
T1 south side of valley	492–510	Paired and poorly preserved	Highly weathered silty clay with manganese oxide and iron oxide mottling	2.5YR 4/6	Water-rolled cobbles and gravels fine upwards (a-axis of up to 70 cm), limestone, volcanic, and metavolcanic composition
T1 north side of valley	492–510	Paired	Highly weathered silty clay extends for 315 m	10YR 5/8	Remnants of pyroclastic flow, boulders of volcanic ejecta (a-axis of up to 1.40 m), and scoria all found on top of the terrace
T2	485–488	Unpaired by Liang Bua	Brown slopewash merges into highly weathered silty clay with iron oxide mottling	10YR 5/6	Numerous weathered clasts of limestone and volcanic origin nodules of weathered charcoal, fine upwards
T3	480–475	Unpaired	Clayey sand with sharp iron oxide layer	7.5YR 5/4	Dense concentration of volcanic and limestone clasts (some with a maximum a-axis of up to 1 m) towards the base

age range for this terrace of 250–215 ka, suggesting that the river occupied the same elevation as the cave  $\sim 200$  ka. It subsequently eroded its floodplain over the next 100 k.yr., reaching the elevation of the second terrace at  $18 \pm 4$  ka (sample WR-13) followed by the third terrace during the Holocene at  $5 \pm 2$  ka (sample WR-1) (Fig. 7).

The presence of a largely eroded first terrace on the southern side of Wae Racang valley, and a well-preserved corresponding terrace on the opposite side of the valley, suggests that the river had wandered across to the southern side of the valley  $\sim 200$  ka, prior to terrace formation. A layer of pyroclastic deposits that had previously formed a capping over the third terrace, aided its

preservation on the northern side of the valley, as suggested by the remaining volcanic boulders and scoria (Fig. 3h, white dashed circles, Fig. 6). This terrace represents an overbank deposition of the former river with a maximum age of  $\sim 215$  ka, and a section of imbricated gravel deposited at the edge of the main channel wandered across to the southern valley.

The extensive preservation of the second terrace on the southern side of the river, and its degree of erosion on the northern side, suggests that when the river occupied this elevation at  $\sim 20$  ka it had returned to the midpoint in the valley, close to the present location of the river, and any further movement northwards was

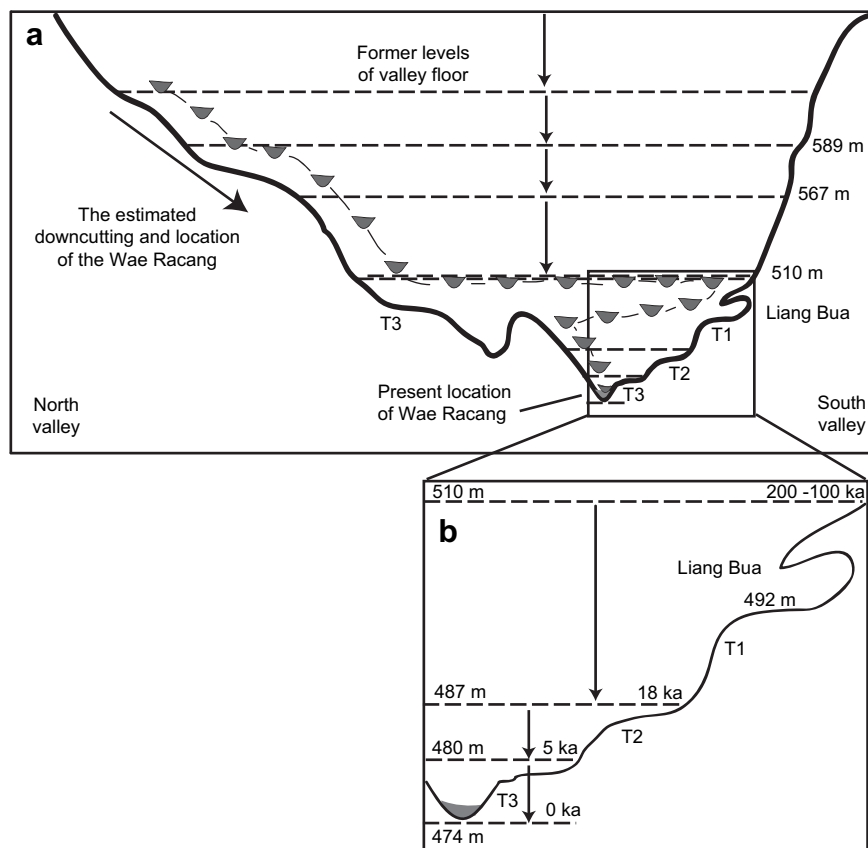


**Figure 7.** A reconstruction of the river and terraces in Wae Racang valley. (a) The estimated location of the Wae Racang during alluvial downcutting of the valley, based on the sedimentology and structure of the alluvial terraces. The semi-circles represent the former locations of the river, the solid grey line represents the present valley profile, while the dashed lines represent the estimated former levels of the valley floor. This schematic demonstrates that at one time the river was situated in close proximity to the subterranean chamber of Liang Bua. (b) The height above sea level and the age of the terraces are based on results presented in Westaway (2006) and Roberts et al. (2009) and in Fig. 6.

obstructed by the capped first terrace and karst cone. This barrier caused the concentration of alluvial erosion after ~18 ka, which subsequently completely removed the second terrace from this location (Fig. 3d). The sedimentological characteristics of this terrace on the southern side provide evidence for this river movement as the coarser units found towards the lower sections represent a central channel location before the river moved, and the overbank and mass movement deposits in the upper sections of the terrace represent a backwater fluvial environment, and were deposited after the river had moved northwards (Fig. 7).

The combined sedimentological and chronological evidence suggests that at ~200 ka the river was occupying the southern side of the Wae Racang valley. The incision by the river into its former floodplains and bedrock created a series of terraces and established a vertical incision rate of 36 m over a period of ~100 k.yr., which provides evidence for the erosive abilities of the Wae Racang. This information provides vital clues for determining the age of cave exposure.

**The pattern of cave collapse** When caves are formed entirely by solution, their roofs and walls are more vulnerable to the process of collapse (White and White, 1969), and the soft, impure, tuff-bearing clastic limestones of this region facilitate high densities of solution features. In addition, tectonic uplift encourages valley deepening and weakens the structure of dissolution chambers, which is the primary cause of collapse in this landscape. Evidence of this process can be observed in the sediments of Liang Bua at ~5 m (Morwood et al., 2009), where the presence of huge limestone blocks suggest that the cave entrance underwent further collapse. This process was important for initiating the accumulation of archaeological evidence as it transformed a discrete opening into a wide entrance, thereby creating an environment suitable for human occupation.

**The age of the alluvial conglomerate deposits** An extensive alluvial conglomerate dominates the southern end of Liang Bua (Figs. 3l, m, and 8a,b), extending 18 m from the rear wall, with remnants stretching from the west to the east walls, as previously described in Westaway et al. (2007a). The volume of this deposit, its location, and the caliber and composition of its clasts indicate high-energy fluvial transport and deposition of allogenic sediments. The deposition of these fluvial sediments represents the first exposure of the cave by the Wae Racang, so establishing their depositional age is essential for determining the age of chamber exposure. The conglomerate cliff exposure can be divided into three sedimentary layers: basal, middle, and upper (Westaway et al., 2007a). The TL ages for the basal conglomerate ( $193 \pm 33$  ka, sample LBC-36) and upper conglomerate ( $130 \pm 57$  ka, sample LBC-37) indicate that sub-aerial exposure of the cave occurred no earlier than the late Middle Pleistocene (Westaway et al., 2007a; Roberts et al., 2009), which agrees with the age range of the first alluvial terrace at ~200 ka. The basal unit contains an upward-fining sequence that represents a flood deposit and the initial exposure, while the deposition of the middle and upper units can be attributed to the erosion and reworking of the basal conglomerate from the back of the sloping rear chamber towards the front. Thus, the age of ~190 ka is viewed as being a maximum age for the exposure of Liang Bua, while the age of ~130 ka represents a maximum age for the deposition of the reworked upper conglomerate.

#### *Implications for the archaeology of Liang Bua*

Liang Bua was a subterranean chamber for at least ~400 k.yr. before it was exposed to form a cave at ~190 ka. This evidence suggests that the chamber must have accumulated at least 400 k.yr. of pre-occupation sediments before river exposure and deposition

of the conglomerate deposits. This information is important for interpreting the sediments in Liang Bua (Westaway et al., 2009a) and distinguishing between the sediments deposited pre-occupation and those deposited during occupation. The lithology of soft limestone, the density of solution features, and the effects of uplift have contributed to the high occurrence of collapse in this landscape, which has, in turn, contributed to the creation of environments that could be occupied. Sedimentological evidence from the terraces suggests that the river was situated at an altitude of ~150 m in the southern valley at ~200 ka (or the equivalent of ~430 m when taking into account the uplift since 200 ka), when the river deposited sediments inside the cave at ~190 ka by exposing the front entrance. This event represents a maximum age for the occupation of Liang Bua. As stone artifacts were discovered embedded in the middle and upper layers of the north-facing wall of the conglomerate (Morwood et al., 2004; Westaway et al., 2007a), this age also corresponds to the initial deposition of the artifacts, and represents a minimum age for hominin occupation of western Flores.

#### **The evolution of the site**

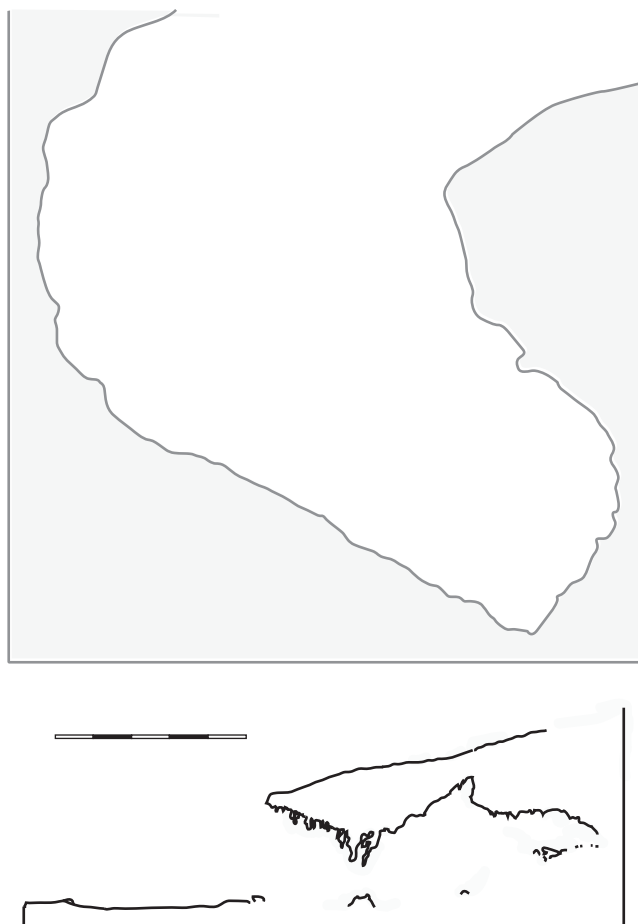
Since its formation at ~600 ka, Liang Bua has evolved from a subterranean chamber into an exposed, semi-collapsed, interconnected multi-level cave. Evidence for this evolution can be gained from; (1) the pattern of cave development in this region; (2) the dominance of tectonic uplift and the pace of river downcutting; and (3) collapse depicted by speleothem precipitation. These developments have implications for the distribution of archaeological material discovered at the site.

#### *The pattern of cave development*

The evolution of Liang Bua from subterranean chamber to its present day form did not occur in isolation but rather as an integral part of a large cave system. The Wae Racang river valley in the vicinity of Liang Bua contains four separate multi-level and interconnected cave systems over a horizontal distance of ~3 km, similar to the Demanovska caves in Czechoslovakia (Droppa, 1966), and the caves of the Guizhou province in southwest China (Jones et al., 2004). The morphology of these cave systems indicates the dominant pattern of cave evolution.

The Liang Bua cave system is interconnected via a series of passages and sinkholes, which form a cave system that stretches for 550 m and covers a total elevation of 138 m, and includes Liang Tanah, Liang Bua Outcrops I and II and the subterranean chamber, and Liang Jama and Longkajama. It is connected to the other caves in the system at five entry points, outlined in Fig. 8a: a passage connecting to Liang Tanah, a smaller domed solution chamber situated at a slightly higher altitude, enabling water and slopewash to be channeled into Liang Bua (Fig. 8a, "1"); a sinkhole, a small cave/passage, and a large sinkhole at the rear of the cave that connects to Liang Bua Outcrops I and II (Fig. 8a, "2–4," respectively); and a sinkhole at the rear of the cave that connects to the subterranean chamber at the base of the cave system (Fig. 8a, "5"). This basal chamber receives subterranean water flow from the other caves in the system, either storing this water as a pond or channeling it through the landscape to the water table. Within this area, caves containing large solution chambers are either stacked on top of each, or found at a similar elevation, and are generally located at lower altitudes relative to the other caves. In contrast, caves with a dense network of narrow passages are generally situated at higher altitudes. This suggests that the latter caves tend to channel water and slopewash, whereas larger solution chambers tend to accumulate pond water until a new series of caves are developed at





relates to the agents of erosion and deposition within the cave sediments, e.g., sinkholes and connecting passages can form channels creating pooling and cut and fill stratigraphy.

The rear and front chamber in Liang Bua, extending 18.7 m and 15.8 m, respectively, also illustrates the influence of tectonic uplift over chamber evolution. Differences in the form of these chambers indicate that their evolution has been influenced by the deepening river valley, which has progressively reduced the distance of the cave in relation to the ground surface (Westaway et al., 2007a) causing the form of the chambers to reflect the mechanical response of rock at that depth (Bogli, 1980; Jennings, 1985). The elliptical form of the rear chamber suggests it evolved deep within the bedrock where the rock has a plastic form (Bogli, 1980), and this form was maintained despite further uplift (Fig. 9a). In contrast, the domed form of the front chamber suggests it was formed later, assisted by the elastic properties of rock at shallower depths and the pattern of uplift at that time, which enabled the formation of a large domed profile (Fig. 9b). This form would have also contained a correspondingly domed basin with the potential to accumulate deep cave sediments. The domed front chamber, therefore, has accumulated over 16 m of sediment, while the rear chamber has accumulated a much smaller proportion. Due to the effects of uplift between the two cave forming periods, the younger domed chamber was formed approximately 14 m lower than the older rear chamber, which created a cliff-like junction between the chambers that runs across the center of the cave (Fig. 8a, dashed line). During its subterranean evolution, the domed front chamber would have occasionally accumulated water from the rest of the cave system, in a similar manner to the present subterranean chamber. This scenario is consistent with the morphology of the cave system (Fig. 5), the evolution of the chambers (Figs. 8 and 9), and the sedimentology of the basal cave sediments (Morwood et al., 2009; Westaway et al., 2009a).

#### *Collapse depicted by stalactites*

The pattern of stalactite precipitation in Liang Bua is an additional source of evidence for the evolution of the cave by the process of collapse. When a subterranean chamber is exposed, the form of stalactite precipitation is affected by evaporation, as the exposed side loses carbon dioxide more rapidly, causing greater calcite precipitation. Small bacteria and phototrophic organisms living within the calcite assist this process by increasing the loss of

a lower altitude. This evidence provides clues as to how and why Liang Bua evolved into its present-day form.

#### *The dominance of tectonic uplift*

Tectonic uplift in the region controls the pace of cave evolution and creates distinct multi-level cave morphologies caused by a constantly descending palaeowater table. This water level keeps pace with uplift so that the “cave forming level” is shifted to a lower altitude. Solution processes respond to this change in base level by the downward extension of the cave system via phreatic tubes and sinkholes creating a new level in this cave system, and the abandonment of dissolution chambers at higher altitudes. The importance of this multi-level and interconnected nature relates to the source area of the sediments; for example, sediments and water can be channeled from any of the other caves in the system. It also

carbon dioxide, thereby causing increased precipitation towards the source of the sunlight (Finlayson and Hamilton-Smith, 2003). The stalactites found in the center of the domed front chamber in Liang Bua display extreme phototrophism (Fig. 31 – red dashed lines), but this effect decreases in an easterly and northerly direction, with the straightest stalactites occurring in the less exposed rear elliptical chamber (Fig. 31 – black dashed lines). This evidence implies that the first exposure would have occurred in the center of the cave and would not have been extensive. Over time, the transformation of this small opening into a wide entrance would have increasingly affected the northern and eastern sides of the newly formed entrance.

#### *Implications for the archaeology of Liang Bua*

The evolution of Liang Bua into a multi-level and interconnected cave system would have initiated sinkhole action causing the introduction of large amounts of water channeled through the cave environment in the form of channels, pools, and sheetwash. These processes would have been especially apparent during the wet seasons and during large storm events. This information has implications for the interpretation of the stratigraphy and occupation phases in Liang Bua, which would have undoubtedly been affected or restricted by this intrusion. Furthermore, these processes may have eroded many of the archaeological deposits, thereby limiting the preservation of evidence and making the presence of erosion contacts in the sediment column an important feature for interpretation.

The relative difference in height between the two chambers would have made the front chamber more accessible for occupation, and its accumulation of deeply stratified sediments provides a potentially rich source of archaeological evidence. Furthermore, the development of the domed front chamber would have encouraged pond formation. Therefore, despite the exposure of the cave occurring at ~190 ka, the evolution of the chamber may have occasionally created an environment that was not conducive to occupation, such as a profusion of ponds and channels. In addition, the evidence from the precipitation of stalactites suggests that the initial exposure would not have been extensive, and it would have been many thousands of years before the mouth of the cave was transformed into a wide entrance that was conducive to occupation.

#### **The external influences on the site**

Since ~190 ka, when the cave was first exposed, Liang Bua has been subjected to a number of external influences: geomorphological, volcanic, environmental, and climatic, which have been fundamental in modifying the form of the cave and altering the occupational environment.

#### *Geomorphological and volcanic influences*

After the initial exposure event, evidence from the height and age of the terraces (see “The age of the site” above) suggest that despite constant downcutting, the river would have been able to reach the level of the cave entrance by overbank flooding. This provided a long period of potential inundation where the river (or a smaller tributary of the river) could influence the geomorphological development of the cave by eroding, depositing, and creating pools (Westaway et al., 2009a). In addition, sedimentary evidence from Liang Bua indicates that volcanic activity occurred at ~17 ka and 12 ka, which deposited airfall sands and tephra in the sediment column and infiltrated the water supply in the cave environment (Westaway et al., 2009a, b).

#### *Palaeoenvironmental influences*

As the potential occupation period for Liang Bua spans three transitions from glacial to interglacial cycles, the palaeoclimate influences on the cave would have been significant. Evidence for the palaeoclimate changes that occurred in the IPWP region for some of this period have been derived from the  $\delta^{18}\text{O}$ ,  $\delta^{13}\text{C}$ , and fluorescence values of a stalagmite from Java (SPJ3 – Fig. 10). Despite being precipitated on a different island, this stalagmite closely correlates with the  $\delta^{18}\text{O}$  and  $\delta^{13}\text{C}$  values and growth rates (Fig. 10c) from stalagmites found on Flores (Westaway, 2006; Westaway et al., 2007b), but in contrast, SPJ3 also contains a strong fluorescence signal, which is a useful proxy for humification and effective precipitation (Baker and Genty, 1999; McGarry and Baker, 2000). For proxies such as fluorescence and  $\delta^{13}\text{C}$  that generally reflect localized conditions above the cave, these data can only be used as a rough indication of the conditions on Flores, but their correlation with  $\delta^{18}\text{O}$  data and growth rates from Flores suggest that their use is not unwarranted.

The details of the region, cave, sampling site, and stalagmites can be found in Westaway et al. (2007b), and in the SOM. As the speleothem isotopic variability is influenced by a number of complex processes occurring in the rainwater, vegetation, soil water, soil, and cave atmospheres, the following interpretations, based on estimated relationships between isotopic values and climate conditions (outlined in the SOM), are limited by a degree of uncertainty. To overcome these uncertainties we have correlated between six separate proxies:  $\delta^{18}\text{O}$ ,  $\delta^{13}\text{C}$  (Fig. 10a), growth rate (Fig. 10c), physical characteristics (Westaway et al., 2007b), tonal intensities (Fig. 10a), and fluorescence wavelength and intensity (Fig. 10b), and combined the results for testing the integrity of the samples (Westaway et al., 2007b) to identify six separate periods of climatic change (Fig. 10a: 1–6). The rate and potential magnitude of these changes was likely to be significant enough to influence human sustainability at the site.

#### *Period 1: 49–39 ka, wet and organic rich*

Fast growth rates fuelled by increases in soil water during this period (Fig. 10c) indicate that Eastern Indonesia received high effective precipitation over the cave catchment areas, and the soil  $\text{CO}_2$  and carbonate concentration in the drip water were high, indicating increased bio-productivity and a consistent supply of groundwater, respectively. In addition, the growth layers contain relatively high emission intensities and long emission wavelengths indicating that the organic matter was washed out of the soil, which restricts the breakdown of complex long chain organic molecules and the degree of humification (Baker and Genty, 1999) and increases levels of humic-like compounds in the stalagmite. This evidence indicates a generally wet environment due to a strong monsoon, and as fast growth rates (21–84  $\mu\text{m}/\text{yr}$ ) correlate with low  $\delta^{18}\text{O}$  values it also indicates increased effective precipitation (Fig. 10a, c). This wet climate was especially apparent between 44–41 ka, when the fluorescence and  $\delta^{18}\text{O}$  data displays two rapid shifts during the precipitation of fast growing, organic-rich layers (Fig. 10a, b).

#### *Period 2: 39–36 ka, transitional phase – decreasing rainfall*

All proxy-records display a large shift, suggesting that this period represents a transitional climatic phase. The growth rate significantly decreases, the calcite layers are darker (Fig. 10c), indicating an influx of less organic impurities, and the  $\delta^{13}\text{C}$  record shifts to higher values, indicating a decrease in effective precipitation and/or a gradual shift to  $\text{C}_4$  grasses (see the SOM). The

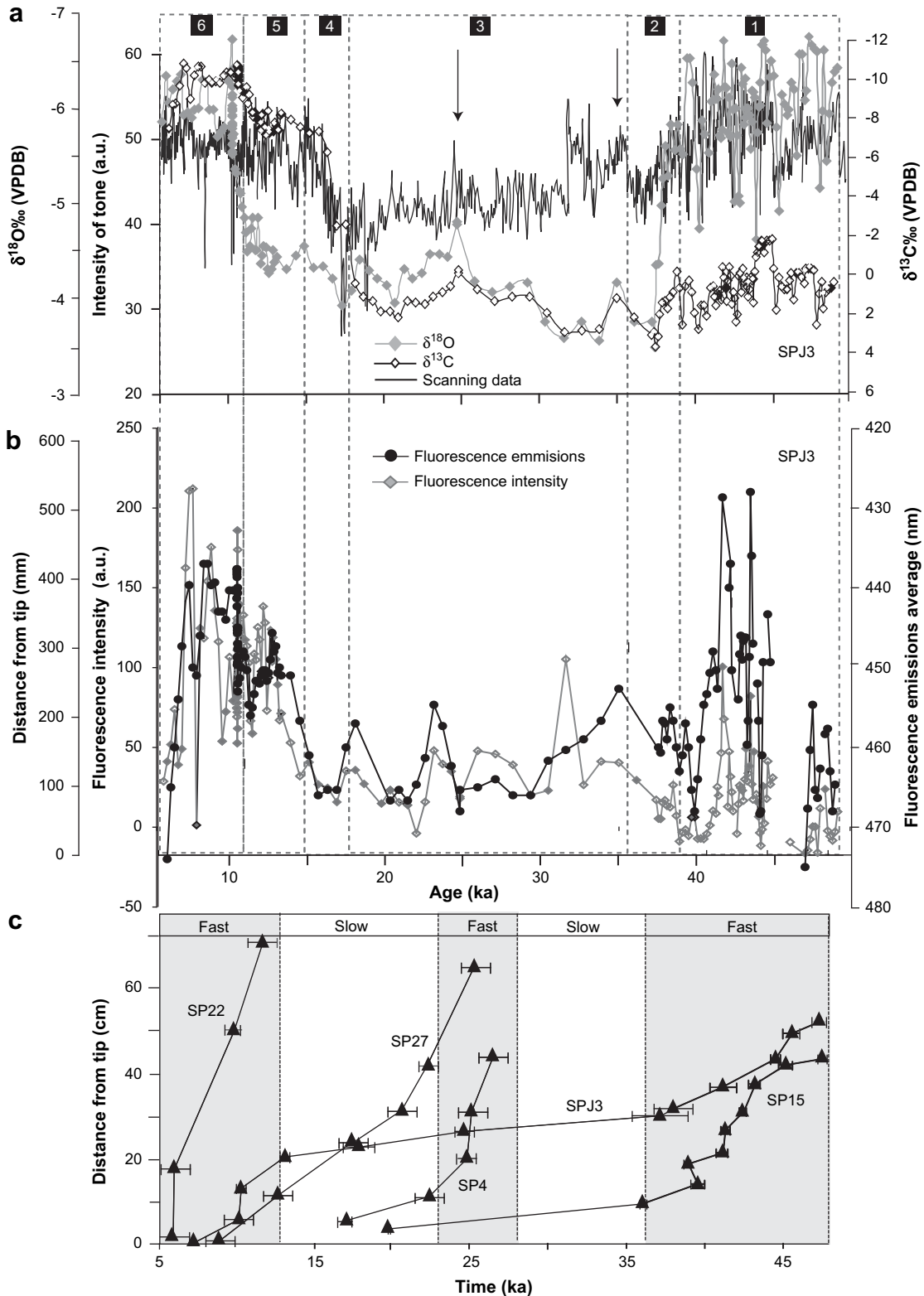


**Figure 10.** A comparison of different proxies within the speleothem records from Flores and Java. (a) A comparison of the tonal intensity of the growth layers, as determined by the scanning data (black lines), with the  $\delta^{18}\text{O}$  (filled grey diamonds) and  $\delta^{13}\text{C}$  (open black diamonds) values for sample SPJ3 from Java. The carbon isotope data can be read from the right axis, while the oxygen isotope and scanning data can be read from the left axis. (b) A comparison of the fluorescence emission (black circles) and intensity (grey diamonds) for sample SPJ3 from Java. The intensity data can be read from the left axis, while the emission data can be read from the right axis. Note the break in emissions at  $\sim 45$  ka represents an absence of data for that period. (c) A comparison of the growth rates for five stalagmite records from Flores (SP4, SP27, SP22, and SP15) and SPJ3 from Java (Westaway et al., 2007b), which display a general agreement in growth rate patterns. The growth rates have been loosely grouped into fast growth (grey shading) and slower growth (no shading), but the stalagmites from Flores generally display much faster rates than Java from  $\sim 25$  ka onwards. These data sets (a, b, c) have been plotted on the same scale so that direct correlations can be made between the six proxy data sets. Six significant isotopic shifts have been marked on (a) and (b) with grey dashed boxes (numbered 1–6). The scanning (a), fluorescence (b), and growth rate data from Flores and Java (c) all agree with this model of climate change. The two vertical arrows denote rapid shifts from climatic stability at 35 ka and 25 ka, as discussed in the text.

fluorescence wavelengths shorten and intensity decreases, implying an increase in humification and organic matter and a longer residence time in the soil due to a reduction in rainfall and soilwater (although the slower growth rate would also act to concentrate organic compounds). The inferred decrease in rainfall implies a weakening of the monsoon system and a reduction in rainfall due to a shift to a more isotopically enriched moisture source (Westaway et al., 2007b).

#### Period 3: 36–17 ka, dry but stable conditions

During this extended dry period, the conditions stabilized with no large fluctuations, the growth rates remained slow from 38 ka to 22 ka, reaching a minimum between 22–17 ka (Fig. 10c), while the tonal intensities reflect slow growing, organically-poor layers (Fig. 10a). The shift to low rainfall was maintained throughout this period ( $\delta^{13}\text{C}$  and  $\delta^{18}\text{O}$  remain enriched) (Fig. 10a) implying that the monsoon remained weak due to the reduced movement of the ITCZ. There was an extended phase of humification in a dry environment, a decrease in the availability of soil organic matter (shorter fluorescence wavelengths and low intensity fluorescence emissions) (Fig. 10b), and a possible increase in  $\text{C}_4$  grasses (van der Kaars and Dam, 1995). The only deviations from this stability were rapid shifts at  $\sim 35$  ka and  $\sim 25$  ka, which can be observed within four of the records (Fig. 10a, vertical arrows), with the latter shift also reflected in an increase in growth rates on Flores (Fig. 10c). A large concentration of hiatuses in the speleothem calcite towards the start of this period indicates a reduction in the soil  $\text{CO}_2$ , which is consistent with a reduction in vegetation and the extent of rainforest cover (Wyputta and McAvaney, 2001). The glacial maximum at  $\sim 18$  ka caused a large decrease in effective precipitation in the tropics (De Deckker et al., 1991; Kershaw et al., 2001; Keast, 2001) by as much as 30% (Wyputta and

McAvaney, 2001), a decrease in humidity (Whitmore, 1981), increased seasonality (Whitmore, 1981; Morley and Flenley, 1987), and a lowering of the tree line (Whitmore, 1981; Morley and Flenley, 1987; van der Kaars et al., 2000; Keast, 2001). In addition, this drier climate caused a reduction in lake levels (Dam et al., 2001), and an increase in desert environments (Whitmore, 1981; van der Kaars and Dam, 1995; van der Kaars et al., 2000; van der Kaars, 2001; Dam et al., 2001; Hope, 2001; Penny, 2001). This evidence suggests the presence of an open landscape, which is supported by the incidence of diurnal raptor fossils within Liang Bua sediments (Meijer, 2006; van den Bergh et al., 2009).

#### Period 4: 17–15 ka, transitional – increasing rainfall

This period represents another transitional phase, but of environmental recovery rather than deterioration. Although the speleothem growth rates remained generally slow (but slightly faster on Flores), the fluorescence wavelengths,  $\delta^{13}\text{C}$  values, tonal intensities, and scanning data display a large, rapid excursion between 17–15 ka, signifying a transition into wetter climates (Fig. 10, period 4). The magnitude of this excursion could represent an increase in effective precipitation that resulted in an increase in vegetation, particularly  $\text{C}_3$  vegetation, such as tropical montane and lowland forest taxa, e.g., Pteridophyta and Dipterocarpaceae (van der Kaars and Dam, 1995), which in turn affected the partial pressure of  $\text{CO}_2$  in the soil. Just prior to this increase, the tonal intensities of the growth layers display two large influxes of inorganic material, representing an increase in slope-wash above the cave (Fig. 10a). This increase in soilwater corresponds to only a small decrease in  $\delta^{18}\text{O}$  values, as the rainfall in this region is still being dominated by the enriched moisture source. During the later part of this period, the shift towards shorter fluorescence wavelengths could indicate a gradual increase in soil temperatures.

**Table 2**

Summary of the climatic and environmental changes inferred from the palaeoenvironmental analysis of stalagmite SPJ3 from Java with growth rate evidence from stalagmites on Flores.

Period	Time (ka)	Proxy evidence	Inferred climatic and environmental conditions	Possible interpretation of environmental conditions	Influences on occupation
1	49–39	Fast growth rates, $\delta^{18}\text{O}$ fluctuating but mainly depleted, $\delta^{13}\text{C}$ gradually increases to enriched, long fluorescence wavelengths and low intensity, high tonal intensities	Wet and organically-rich	Closed woodland conditions, unstable with rapid fluctuations in rainfall	Wide range of vegetation, large supplies of water
2	39–36	Fast growth rates, short wavelengths and low intensity, $\delta^{18}\text{O}$ and $\delta^{13}\text{C}$ increasing, layers darken	Transitional – decreasing rainfall	Gradual reduction in rainfall and shift to $\text{C}_4$ vegetation	Reduction in water supply, certain vegetation food sources decreasing
3	36–17	Slow growth rates but briefly increase at 25 ka, $\delta^{18}\text{O}$ and $\delta^{13}\text{C}$ enriched, with a decrease at 25 ka, short fluorescence wavelengths and low intensity, low tonal intensities	Dry and organically-poor but stable	Open landscapes – less tree cover, decrease in soil organic matter, increase in $\text{C}_4$ vegetation, decreasing humidity, increasing seasonality, lowering of tree line, reduction in rainforest cover and lake levels, shift towards more grassland and desert environments	Low water supplies, change in vegetation causing a change in fauna? Less rainforest cover affecting hunting activities?
4	17–15	Slow growth rates, and $\delta^{13}\text{C}$ significant excursion to depleted values, $\delta^{18}\text{O}$ stays enriched, rapid shift to longer fluorescence wavelengths, two rapid shifts to lower intensity	Recovery I – Increase in rainfall	Rapid shift to wetter climates, increase in montane and lowland forest taxa, increase in soil temperatures, volcanic activity	Increase in water availability, certain vegetation food sources increasing but affected by volcanic ash?
5	15–11	Growth rates increase, $\delta^{18}\text{O}$ excursion to depleted values, smaller $\delta^{13}\text{C}$ excursion to depleted values, short fluorescence wavelengths and intensity increasing, tonal intensity increases	Recovery II – The return of the monsoon	Closed canopy conditions – Increase in soil thickness and shift to monsoonal seasons, volcanic activity	Wide range of vegetation, large supplies of water but infiltrated by ash?
6	11–5	Fast growth rates, $\delta^{18}\text{O}$ and $\delta^{13}\text{C}$ depleted, long fluorescence wavelengths and high intensity, high tonal intensity	Stabilizes into early Holocene, wet and organically-rich	Wet conditions – increase in humid forests, increased soil temperatures and humidity, increase in ENSO activity	Wide range of vegetation, large supplies of water, increase in flooding and forest fires?

*Period 5: 15–11 ka, transitional –*

During this period, the growth of vegetation began to increase, indicating the thickness and soil water in response to increased rainfall. The fluorescence shifts to shorter wavelengths, suggesting that although the environment was still recovering after the LGM, a small decrease in temperature and humidity reduced the rapidity of this recovery. Similar to the LGM, the decrease in effective rainfall increases, but the rapidity or magnitude as seen in the previous period. Vegetation has already been established. This is supported by the first appearance of parrots in the fossil record before ~12 ka that favor closed canopy environments (Bergh et al., 2009). During the later part, at ~13 ka, δ<sup>13</sup>C values decreased, which has been interpreted as a return to a signal depleted moisture source and an indication of environmental recovery. The timing of this shift coincides with the re-establishment of the monsoon system by 14 ka, due to movement of the ITCZ (Vyrwoll and Miller, 2001).

*Period 6: 11–5 ka, wet and relatively stable*

This period of low δ<sup>13</sup>C values represents the stabilization of the environment (Fig. 10, period 6). The peak emission wavelength decreased during the initial part, reflecting increased soil temperatures from 10 ka to 8 ka, and then returned to longer wavelengths, indicating wetter conditions into the Holocene. The increase in rainfall caused a large increase in humid conditions (Bergh et al., 2009). The decrease in δ<sup>13</sup>C values is consistent with the increase in δ<sup>13</sup>C values (due to the increase in rainfall) (Gagler et al., 2012; Gagler et al., 2013).

changes and unstable climatic conditions over short timescales that would also have caused rapid changes in food supplies and forced migrations to new areas. In addition, volcanic activity appears to have been a major influence on the site, affecting vegetation, fauna, and water supplies (Westaway et al., 2009a, b). As these influences affected hominin activities, they would also have affected the distribution of archaeological material (e.g., causing increases or absences), and must, therefore, be considered during interpretation of the evidence.

## Summary

Evidence for the geological, tectonic, and climatic histories of Flores provide the basis for reconstructing the formation, age, evolution, and influences on Liang Bua. The formation of Liang Bua as a subterranean chamber at ~600 ka precluded occupation but allowed at least 400 k.yr. of pre-occupation sediments to accumulate. At ~200 ka the Wae Racang wandered across to the southern side of the valley where, assisted by the soft nature of the limestone and the dominance of collapse processes, the river exposed the cave entrance and deposited a conglomerate containing artifacts at the rear of the cave at 190 ka (Fig. 11). This evidence provides a maximum age for human occupation of the site and a minimum age for the human occupation of the area. The evolution of this subterranean chamber into a multi-level and interconnected cave resulted in modifications to the cave environment by sinkhole channeling and ponding, which affected the potential for occupation and preservation of archaeological material. The evolution of the two chambers during uplift created different chamber morphologies, with different degrees of accessibility and accumulation of archaeological material. Glacial phases were responsible for changes in local vegetation, fauna, and hominins, but volcanic activity and the influence of the flooding river would have also impacted on the cave environment. In this respect, the timing of these landscape and environmental changes represent important contextual information that has implications for the interpretation of the archaeological evidence found in Liang Bua.

## Acknowledgements

This study was funded by a Discovery Project grant to M.J.M. from the Australian Research Council (ARC), with additional funding to R.G.R. from the University of Wollongong. We also thank the ARC for a Senior Research Fellowship to R.G.R.; E.W. Saptomo and colleagues at the Centre for Archaeology (Jakarta) for logistical support in Flores and Java; H. Scott-Gagan for stable isotope measurements conducted at the Australian National University and useful discussion; R. Drysdale for ideas relating to scanning and tonal intensities and useful discussions; D. Wheeler for stable isotope measurements conducted at the University of Wollongong; Y.-x. Feng for U-series measurements; T. Lancaster, D. Hobbs, Ginardo, and Pa Teguh for field assistance; and P. Westaway and the University of Wollongong (University Postgraduate Award and Tuition Fee-Waiver Scholarship) for financial support of K.E.W.

## Appendix. Supplementary data

Supplementary data associated with this article can be found in the online version, at doi: [10.1016/j.jhevol.2009.01.007](https://doi.org/10.1016/j.jhevol.2009.01.007)

## References

Abbott, M.J., Chamalaun, F.H., 1981. Geochronology of some Banda arc volcanics. The Ecology and tectonics of Eastern Indonesia. *Geol. Res. Dev. Cent.* 2, 253–268.

- Audley-Charles, M.G., 1981. Geological history of the region of Wallace's Line. In: Whitmore, T.C. (Ed.), *Wallace's Line and Plate Tectonics*. Clarendon Press, Oxford, pp. 24–35.
- Baker, A., Genty, D., 1999. Fluorescence wavelength and intensity variations of cave waters. *J. Hydrol.* 217, 19–34.
- Bard, E., Jouannic, C., Hamelin, B., Pirazzoli, P.A., Arnold, M., Faure, G., Sumosusastro, P., Syaefudin, 1996. Pleistocene sea levels and tectonic uplift based on dating corals from Sumba Island, Indonesia. *Geophys. Res. Lett.* 23, 1473–1476.
- Bellwood, P., 1997. *The Prehistory of Indonesian Malaysian Archeology*. University of Hawai'i Press, Honolulu.
- Bogli, A., 1980. *Karst Hydrology and Physical Speleology*. Springer-Verlag, Berlin.
- Burrett, C., Berry, D.R., Varne, R., 1991. Asian and South-western Pacific continental terranes derived from Gondwana, and their biogeographic significance. *Aust. Syst. Bot.* 4, 13–24.
- Chappell, J., Veeh, H.H., 1978. Late Quaternary tectonic movements and sea-level changes at Timor and Atauro Island. *Geol. Soc. Am. Bull.* 89, 356–368.
- Dam, R.A.C., van der Kaars, S., Kershaw, A.P., 2001. Quaternary environmental change in the Indonesian region. *Palaeogeogr. Palaeoclimatol. Palaeoecol.* 171, 91–95.
- Davies, W.E., 1951. Mechanics of cave breakdown. *Nat. Speleo. Soc. Bull.* 13, 36–43.
- De Deckker, P., Corregge, T., Head, J., 1991. Late Pleistocene record of cyclic eolian activity from tropical Australia suggesting the Younger Dryas is not an unusual climatic event. *Geology* 19, 602–605.
- Dennell, R.W., 2004. Hominid dispersals and Asian biogeography during the Lower and Middle Pleistocene, c. 2.0–0.5 Mya. *Asian. Perspect.* 43, 205–226.
- Droppa, A., 1966. The correlation of some horizontal caves with river terraces. *Stud. Speleo.* 1, 186–192.
- Finlayson, B., Hamilton-Smith, E., 2003. *Beneath the Surface*. UNSW Press, Sydney.
- Flenley, J.R., 1997. The Quaternary in the tropics: an introduction. *J. Quatern. Sci.* 12, 345–346.
- Gagan, M.K., Hendy, E.J., Haberle, S.G., Hantoro, W.S., 2004. Post-glacial evolution of the Indo-Pacific Warm Pool and El Niño-Southern oscillation. *Quatern. Int.* 118–119, 127–143.
- Godley, D., 2002. The reconstruction of flood regimes in Southeast Asia from El Niño-southern oscillation (ENSO) related records. In: Kershaw, A.P., David, B., Tapper, N., Perny, D., Brown, J. (Eds.), *Bridging the Wallace line: The Environmental and Cultural History and Dynamics of the Southeast Asian-Australasian Region*. Catena Verlag GMBH, Germany, pp. 229–254.
- Haberle, S.G., David, B., 2004. Climates of change: human dimensions of Holocene environmental change in low latitudes of the PEPIL transect. *Quatern. Int.* 118–119, 165–179.
- Haberle, S.G., Ledru, M.P., 2001. Correlations among charcoal records of fires from the past 16,000 years in Indonesia, Papua New Guinea, and Central and South America. *Quatern. Res.* 55, 97–104.
- Haberle, S.G., Hope, G., van der Kaars, S., 2001. Biomass burning in Indonesia and Papua New Guinea: natural and human induced fire events in the fossil record. *Palaeogeogr. Palaeoclimatol. Palaeoecol.* 171, 259–268.
- Hall, R., 1996. Reconstructing Cenozoic SE Asia. In: Hall, R., Blundell, D.J. (Eds.), *Tectonic Evolution of Southeast Asia*. Geological Society Special Publication, London, pp. 153–184.
- Hall, R., 2001. Cenozoic reconstructions of Southeast Asia and the South West Pacific: changing patterns of land and sea. In: Metcalf, I., Smith, J.M.B., Morwood, M., Davidson, I. (Eds.), *Faunal and Floral Migrations and Evolution in Southeast Asia-Australia*. A.A. Balkema, Lisse, pp. 35–56.
- Hall, R., 2002. Cenozoic geological and plate tectonic evolution of SE Asia and the SW Pacific: computer-based reconstructions, model and animations. *J. Asian Earth Sci.* 20, 353–431.
- Hamilton, W., 1979. *Tectonics of the Indonesian Region*. United States Government Printing Office, Washington.
- Hisheh, S., Westerman, M., Schmitt, L.H., 1998. Biogeography of the Indonesian archipelago: mitochondrial DNA variation in the fruit bat, *Eonycteris spelaea*. *Biol. J. Linn. Soc. Lond.* 65, 329–345.
- Hope, G.S., 2001. Environmental change in the Late Pleistocene and later Holocene at Wanda site, Soroako, South Sulawesi, Indonesia. *Palaeogeogr. Palaeoclimatol. Palaeoecol.* 171, 129–145.
- Jennings, J.N., 1985. *Karst Geomorphology*. Basil Blackwell, New York.
- Jones, H.L., Rink, J.W., Schepartz, L.A., Miller-Antonio, S., Weiwen, H., Yamei, H., Wei, W., 2004. Coupled electron spin resonance (ESR)/uranium-series dating of mammalian tooth enamel at Paxian Dadong, Guizhou Province, China. *J. Archaeol. Sci.* 31, 965–977.
- van Bemmelen, R.W., 1949. The Geology of Indonesia. In: *General Geology of Indonesia and Adjacent Archipelagoes*, vol. 1A. Government Printing Office, The Hague.
- van den Bergh, G.D., Meijer, H.J.M., Rokhus Due Awe, Morwood, M.J., Szabó, K., van den Hoek Ostende, L.W., Sutikna, T., Saptomo, E.W., Piper, P.J., Dobney, K.M., 2009. The Liang Bua faunal remains: a 95 k.yr. sequence from Flores, East Indonesia. *J. Hum. Evol.* 57 (5), 527–537.
- van der Kaars, S., 2001. Pollen distribution in marine sediments from the south-eastern Indonesian waters. *Palaeogeogr. Palaeoclimatol. Palaeoecol.* 171, 341–361.
- van der Kaars, S., Dam, R.A.C., 1995. A 135,000-year record of vegetational and climate change from the Bandung area, West-Java, Indonesia. *Palaeogeogr. Palaeoclimatol. Palaeoecol.* 117, 55–72.
- van der Kaars, S., Wang, X., Kershaw, P., Guichard, F., Arifin Setiabudi, D., 2000. A Late Quaternary palaeoecological record from the Banda Sea, Indonesia:

- patterns of vegetation, climate and biomass burning in Indonesia and northern Australia. *Palaeogeogr. Palaeoclimatol. Palaeoecol.* 155, 135–153.
- Keast, A., 2001. The vertebrate fauna of the Wallacean Island interchange zone: the basis of imbalance and impoverishment. In: Metcalf, I., Smith, J.M.B., Morwood, M., Davidson, I. (Eds.), *Faunal and Flora Migrations and Evolution in Southeast Asia-Australasia*. A.A. Balkema, Lisse, pp. 287–310.
- Kershaw, A.P., Penny, D., van der Kaars, S., Anshari, G., Thamotherampillai, A., 2001. Vegetation and climate in lowland southeast Asia at the Last Glacial Maximum. In: Metcalf, I., Smith, J.M.B., Morwood, M., Davidson, I. (Eds.), *Faunal and Floral Migrations and Evolution in Southeast Asia-Australasia*. A.A. Balkema, Lisse, pp. 227–236.
- Koesoemadinata, S., Noya, Y., Kadarisman, D., 1994. *Geological Map of the Ruteng Quadrangle, Nusatenggara*. Geological Research and Development Centre, Bandung.
- Kopp, H., Flueh, E.R., Peterson, C.J., Weinrebe, W., Wittwer, A., Scientists, M., 2006. The Java margin revisited: evidence for subduction erosion off Java Earth Planet. *Sci. Lett.* 242, 130–142.
- McGarry, S.F., Baker, A., 2000. Organic acid fluorescence: applications to speleothem palaeoenvironmental reconstruction. *Quatern. Sci. Rev.* 19, 1087–1101.
- Meijer, H.J.M., 2006. *Avifauna of Liang Bua, Flores: Preliminary Report*. Vrije Universiteit, Amsterdam, the Netherlands.
- Monk, K.A., De Fretes, V., Reksodiharjo-Lilley, G., 1997. The Ecology of Nusa Tenggara and Maluku. In: *The Ecology of Indonesia Series*, vol. V. Periplus Editions, Singapore.
- Morley, R.J., Flenley, J.R., 1987. Late Cainozoic vegetational and environmental changes in the Malay archipelago. In: Whitmore, T.C. (Ed.), *Biogeographical Evolution of the Malay Archipelago*. Clarendon Press, Oxford, pp. 50–59.
- Morwood, M.J., Brown, P., Jatmiko, Sutikna, T., Saptomo, E.W., Westaway, K.E., Rokus Awe Due, Roberts, R.G., Maeda, T., Wasisto, S., Djubiantono, T., 2005. Further evidence for small-bodied hominins from the Late Pleistocene of Flores, Indonesia. *Nature* 437, 1012–1017.
- Morwood, M.J., Soejono, R.J., Roberts, R.G., Sutikna, T., Turney, C.S.M., Westaway, K.E., Rink, W.J., Zhao, J.-x., van den Bergh, G.D., Rokus Awe Due, Hobbs, D.R., Moore, M.W., Bird, M.I., Fifield, L.K., 2004. Archaeology and age of a new hominin species from Flores in eastern Indonesia. *Nature* 431, 1087–1091.
- Morwood, M.J., Sutikna, T., Saptomo, E.W., Jatmiko, Westaway, K.E., 2009. Preface: research at Liang Bua, Flores, Indonesia. *J. Hum. Evol.* 57 (5), 437–449.
- Penny, D., 2001. A 40,000 year palynological record from north-east Thailand; implications for biogeography and palaeo-environmental reconstruction. *Palaeogeogr. Palaeoclimatol. Palaeoecol.* 171, 97–128.
- Pirazzoli, P.A., Radtke, U., Hantoro, W.S., Jouannic, C., Hoang, C.T., Causse, C., Borel Best, M., 1991. Quaternary raised coral-reef terraces on Sumba Island, Indonesia. *Science* 252, 1834–1836.
- Pirazzoli, P.A., Radtke, U., Hantoro, W.S., Jouannic, C., Hoang, C.T., Causse, C., Borel Best, M., 1993. A one million-year-long sequence of marine terraces on Sumba Island, Indonesia. *Mar. Geol.* 109, 221–236.
- Roberts, R.G., Westaway, K.E., Zhao, J.-x., Turney, C.S.M., Bird, M.I., Rink, W.J., Fifield, L.K., 2009. Geochronology of cave deposits at Liang Bua and of adjacent river terraces in the Wae Racang valley, western Flores, Indonesia: a synthesis of age estimates for the type locality of *Homo floresiensis*. *J. Hum. Evol.* 57 (5), 484–502.
- Simandjuntak, T.O., Barber, A.J., 1996. Contrasting tectonic styles in the Neogene orogenic belts of Indonesia. In: Hall, R., Blundell, D.J. (Eds.), *Tectonic Evolution of Southeast Asia*. Geological Society Special Publication, No. 106. The Geological Society, London, pp. 185–201.
- Storm, P., 2001a. The evolution of humans in Australasia from an environmental perspective. *Palaeogeogr. Palaeoclimatol. Palaeoecol.* 171, 363–383.
- Storm, P., 2001b. Life and death of *Homo erectus* in Australasia: an environmental approach to the fate of a palaeospecies. In: Sémah, F., Falguères, C., Grimaud-Hervé, D., Sémah, A.M. (Eds.), *Origin of Settlements and Chronology of the Palaeolithic Cultures in Southeast Asia*. Semenajung, Paris, pp. 279–298.
- Tapper, N., 2002. Climate, climate variability and atmosphere circulation patterns in the maritime continent region. In: Kershaw, A.P., David, B., Tapper, N., Penny, D., Brown, J. (Eds.), *Bridging Wallace's Line: The Environmental and Cultural History and Dynamics of the SE-Asian-Australasian Region*. Advances in Geocology. Catena Verlag GmbH, Germany, pp. 5–28.
- Westaway, K.E., 2006. *Reconstructing the Quaternary landscape evolution and climate history of western Flores: an environmental and chronological context for an archaeological site*. PhD Dissertation, University of Wollongong, Wollongong.
- Westaway, K.E., Morwood, M.J., Roberts, R.G., Zhao, J.-x., Sutikna, T., Saptomo, E.W., Rink, J., 2007a. Establishing the time of initial human occupation of Liang Bua, western Flores, Indonesia. *Quatern. Geochronol.* 2, 337–343.
- Westaway, K.E., Morwood, M.J., Sutikna, T., Moore, M.W., Rokus, A.D., van den Bergh, G.D., Roberts, R.G., Saptomo, E.W., 2009b. *Homo floresiensis* and the Late Pleistocene environments of eastern Indonesia: defining the nature of the relationship. *Quatern. Sci. Rev.*, in press.
- Westaway, K.E., Sutikna, T., Saptomo, E.W., Jatmiko, Morwood, M.J., Roberts, R.G., Hobbs, D.R., 2009a. Reconstructing the geomorphic history of Liang Bua: a stratigraphic interpretation of the occupational environment. *J. Hum. Evol.* 57 (5), 465–483.
- Westaway, K.E., Zhao, J.-x., Roberts, R.G., Chivas, A.R., Morwood, M.J., Sutikna, T., 2007b. Initial speleothem results from western Flores and eastern Java, Indonesia: were climate changes from 47 to 5 ka responsible for the extinction of *Homo floresiensis*? *J. Quatern. Sci.* 22, 429–438.
- White, E.L., White, W.B., 1969. Processes of cavern breakdown. *Nat. Speleo. Soc. Bull.* 30, 115–129.
- Whitmore, T.C., 1981. *Palaeoclimate and vegetation history*. In: Whitmore, T.C. (Ed.), *Wallace's Line and Plate Tectonics*. Clarendon, London, pp. 36–42.
- Wyputta, U., McAvaney, B.J., 2001. Influence of vegetation changes during the Last Glacial Maximum using the BMRC atmospheric general circulation model. *Clim. Dyn.* 17, 923–932.
- Wyrwoll, K.-H., Miller, G.H., 2001. Initiation of the Australian summer monsoon 14,000 years ago. *Quatern. Int.* 83–85, 119–128.